Bioorganic & Medicinal Chemistry 17 (2009) 2925–2935

Contents lists available at ScienceDirect

Bioorganic & Medicinal Chemistry

journal homepage: www.elsevier.com/locate/bmc

Design and synthesis of novel dihydroquinoline-3-carboxylic acids as HIV-1 integrase inhibitors

Mario Sechi [a,*], Giuseppe Rizzi [a], Alessia Bacchi [b], Mauro Carcelli [b], Dominga Rogolino [b], Nicolino Pala [a], Tino W. Sanchez [c], Laleh Taheri [c], Raveendra Dayam [c], Nouri Neamati [c,*]

[a] Dipartimento Farmaco Chimico Tossicologico, Università di Sassari, Via Muroni 23/A, 07100 Sassari, Italy
[b] Dipartimento di Chimica Generale ed Inorganica, Chimica Analitica, Chimica Fisica, Università di Parma, V.le Usberti 17/A, Campus Universitario, 43100 Parma, Italy
[c] Department of Pharmacology and Pharmaceutical Sciences, University of Southern California, School of Pharmacy, 1985 Zonal Avenue, PSC 304, Los Angeles, CA 90089, USA

ARTICLE INFO

Article history:
Received 24 June 2008
Revised 29 October 2008
Accepted 31 October 2008
Available online 6 November 2008

Keywords:
HIV-1 integrase inhibitors
Drug design
4-Hydroxy-2-oxo-1,2-dihydroquinoline-3-carboxylic acids
X-ray crystallography

ABSTRACT

Previously, we discovered linomide analogues as novel HIV-1 integrase (IN) inhibitors. Here, to make possible structure–activity relationships, we report on the design and synthesis of a series of substituted dihydroquinoline-3-carboxylic acids. The crystal structure of the representative compound **2c** has also been solved. Among the eight new analogues, **2e** showed a potency in inhibiting IN strand transfer catalytic activity similar to the reference diketo acid inhibitor L-731,988 (IC_{50} = 0.9 μM vs. 0.54 μM, for **2e** and L-731,988, respectively). Furthermore, none of the compounds showed significant cytotoxicity in two tested cancer cell lines. These compounds represent an interesting prototype of IN inhibitors, potentially involved in a metal chelating mechanism, and further optimization is warranted.

1. Introduction

Highly active anti-retroviral therapy, which involves a combination of drugs targeting reverse transcriptase (RT) and protease (PR), remarkably decreases viral load and provides a significant improvement in the life expectancy of HIV/AIDS patients.[1] However, several factors,[2] including the emergence of multi-drug-resistant HIV strains, drug toxicity, the patient's ability to adhere to the prescribed therapy, and costs, are some of the reasons to develop novel drugs targeting other steps in the viral replication process.[3] In this context, HIV-1 Integrase (IN), the enzyme which mediates an obligatory step in the viral replication process by catalyzing the integration of viral cDNA into the host genome, represents a validated target for the development of new drugs against HIV-1 infection.[4–8] IN catalyses the integration process in two steps.[9] In the first step, called 3′-processing, the enzyme cleaves two terminal nucleotides from the conserved 3′-ends of the viral DNA in the cytoplasm of the infected cell. In the second step, after migration into the nucleus of the infected cell as part of a nucleoprotein complex, IN covalently attaches each 3′ processed viral end to the host cell DNA, termed strand transfer. Both 3′-processing and strand transfer are divalent cation-requiring trans-esterification reactions catalyzed by a single active site in the enzyme's catalytic core.

Among all reported IN inhibitors, the β-diketo acids, independently discovered by scientists from Shionogi & Co. Ltd. and Merck Research Laboratories, are the most promising.[10–12] A diketo acid bioisosteric analogue, 5CITEP (Chart 1), was co-crystallized with the enzyme, providing the first X-ray crystal structure of an inhibitor in complex with IN.[13] Meanwhile, other members of the diketo acid family, typified by L-731,988[12] (Chart 1), have been reported and intensively studied.[14–17] Several diketo acid congeners selectively inhibit the strand transfer reaction, and in cell-based assays, they inhibit integration without affecting earlier phases of the HIV-1 replication cycle.[12] It is believed that the β-diketo acid pharmacophoric motif could be involved in a functional sequestration of one or both divalent metal ions in the enzyme catalytic site, to form a ligand-M^{2+}-IN complex, which blocks the formation of the IN-DNA complex by competing with the target DNA substrate.[8] Shionogi/Glaxo-SmithKline's (S/GSK) S-1360[18] and Merck's L-870,810[19] (Chart 1), both belonging to this class of compounds, represent the first IN inhibitors that have entered clinical studies. However, due to pharmacokinetic problems, their development has been stopped. Recently, the diketo acid-based derivative MK-0518[20] (Raltegravir, Chart 1) was approved by the FDA, confirming IN as a rational retroviral drug target. Another compound, the 4-quinolone-3-carboxylic acid GS-9137[21] (Elviltegravir) is in the late stages of clinical development.

* Corresponding authors. Tel.: +39 079 228 753; fax: +39 079 228 720 (M.S.); tel.: +1 323 442 2341; fax: +1 323 442 1390 (N.N.).
E-mail addresses: mario.sechi@uniss.it (M. Sechi), neamati@usc.edu (N. Neamati).

0968-0896/$ - see front matter © 2008 Elsevier Ltd. All rights reserved.
doi:10.1016/j.bmc.2008.10.088

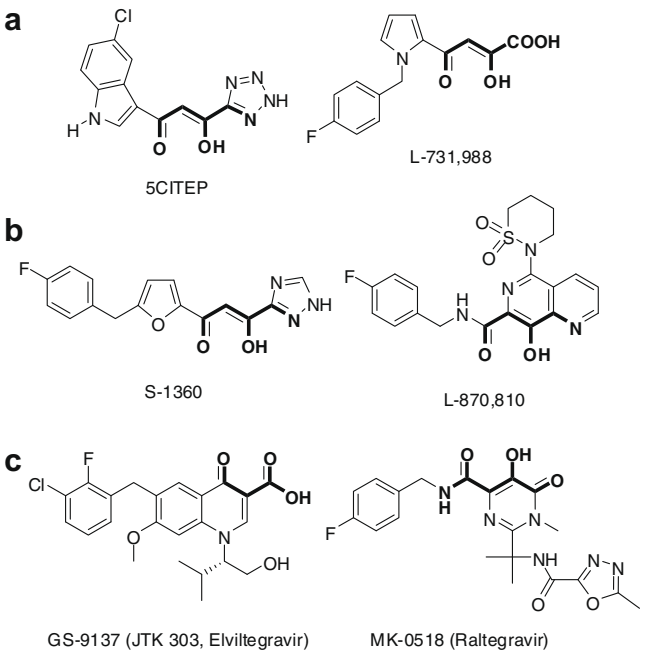

Chart 1. Evolution of β-diketo acid inhibitors: (a) structures of representative diketo acid-based compounds; (b) first compounds entered in clinical trials; (c) HIV-1 IN inhibitors in late stage clinical trials (GS-9137) and recently approved (MK-0518).

There is a great need to discover novel lead compounds with diverse structural scaffolds and promising pharmacokinetic properties, to overcome the difficulties observed with first-generation IN inhibitors. The major progress has been made through high throughput screening, ligand-based computer-aided drug design, and analogue and structure-based pharmacophore modeling methods.[22–32]

Recently, as a part of these studies, we identified a hit, compound **1**, (Fig. 1A),[32] an analogue of roquinimex,[33] that inhibited both 3′-processing and strand transfer activities of IN with IC_{50} values of 40 ± 3 and 16 ± 6 μM, respectively. Further, a limited structure–activity relationship (SAR) study starting from **1** resulted in the identification of several compounds with improved activity.[33] The most potent compound **1a** inhibited both 3′-processing and strand transfer activities of IN with IC_{50} values of 9 ± 5 and 9 ± 4 μM, respectively (Fig. 1B). Contrary to the diketo acid inhibitors, **1a** showed similar inhibitory potency against both 3′-processing and strand transfer. Subsequently, a series of analogues (**2a**–**h**, Fig. 1C) were designed based on a quinolone 3-carboxylic acid pharmacophore hypothesis (Fig. 2). The quinolone 3-carboxylic acid pharmacophore was developed utilizing a training set of compounds including the clinical candidate GS-9137 (Fig. 2).[34] Compounds **2a**–**h** contain the 4-hydroxy-2-oxo-1,2-dihydroquinoline-3-carboxylic acid scaffold **II**, and bear a variety of substituents at 1 (N1) and 6th-position (C6) (Fig. 1C). Herein we report on the design, synthesis, structural studies, and biological evaluation of this new class of IN inhibitors.

2. Results and discussion

2.1. Design

Although several biological and computational studies on diketo acid compounds have been reported,[35–41] the mechanism by which they bind to IN has not been well understood. However, it has been hypothesized to involve direct binding of the diketo acids or diketo acid-type compounds to divalent metal cofactors located on the active site of IN.[8] Several biological studies[40,41] indicate that the inhibitors could interact with the enzyme-viral DNA complex formed after 3′-processing reaction, thus preventing the binding of this complex to the host DNA (Fig. 3A). As previously described,[8,36] the diketo acids and their analogues constitute a prototype of metal chelating inhibitors. In fact, there is structural

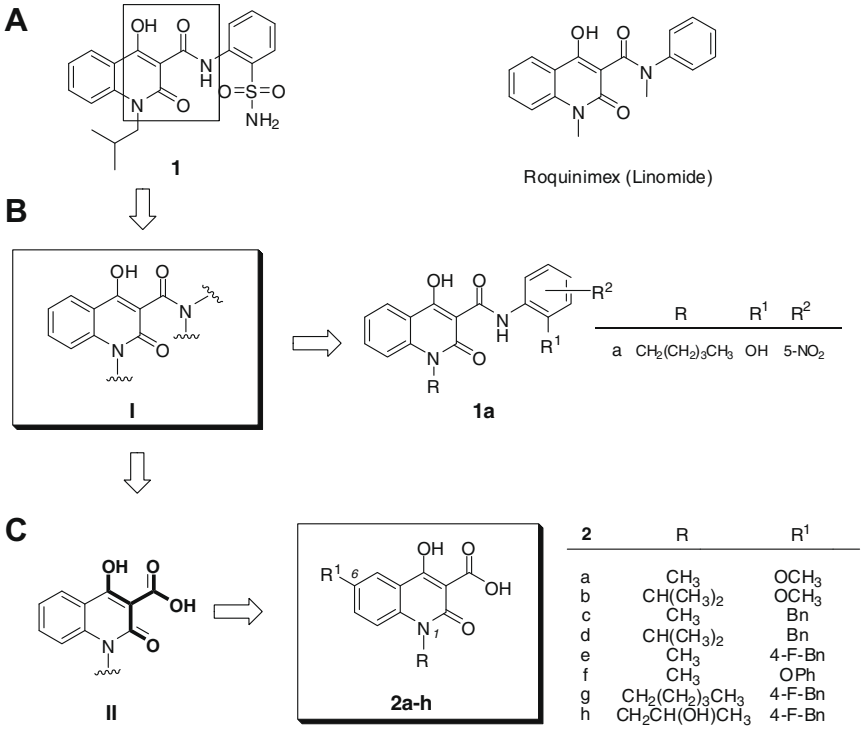

Figure 1. Design of title compounds.

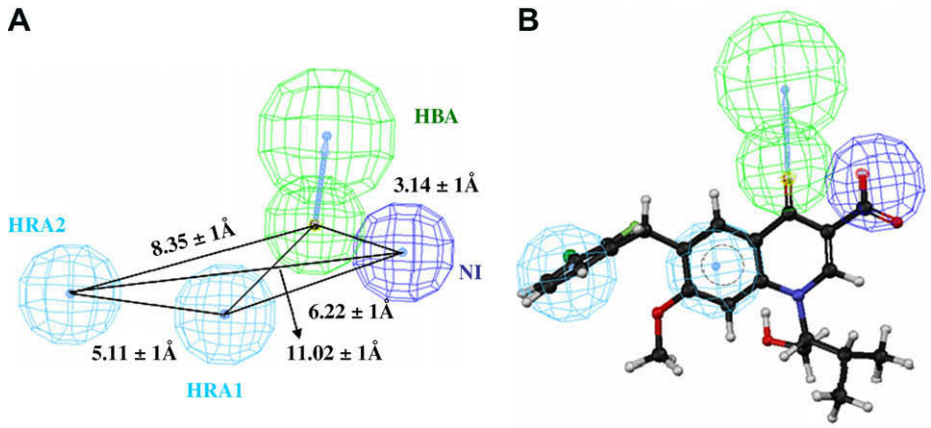

Figure 2. (A) 3D arrangement of four pharmacophore features in the quinolone 3-carboxylic acid pharmacophore. (B) The clinically studied HIV-1 integrase inhibitor GS-9137 is mapped onto the quinolone 3-carboxylic acid pharmacophore. The pharmacophore features depicted as H-bond acceptor (HBA) in green, negatively ionisable feature (NI) in blue and hydrophobic features (HRA1 — 2) in cyan. Interfeature distances are given in angstroms.

evidence that they are able to coordinate metals of biological interest, such as magnesium and manganese.[36] In their ketoenol tautomeric form, these inhibitors present two metal binding sites, the ketoenol and the carboxylate functions (for diketo acids) or the ketoenol and the heteroaromatic rings (for diketo acid-type compounds[42]), which can be involved in coordination with divalent metal ions (Fig. 3B). Considering these facts, we have designed scaffold **II**, by changing the amide of **1a** with the bioisoster acid. Similar to diketo acids and diketo acid-type IN inhibitors, the arrangement of hydroxyl, carboxylate and oxo functional groups on the scaffold **II** could facilitate chelation of two metal ions in the active site of IN (Fig. 3B). Further, a set of analogues (**2a**–**h**, Fig. 1C) with various substitutions on the 6th-position of the scaffold **II** were designed to obtain compounds with optimal fit on the quinolone 3-carboxylic acid pharmacophore. Then, *N*-derivatization with an aliphatic chain has been considered in order to modulate solubility and absorption. Compounds that are mapped onto the quinolone 3-carboxylic acid pharmacophore with high fit value are anticipated to show improved IN inhibitory activity.

2.2. Retrosynthetic analysis and chemistry

The synthesis of the target compounds required access to a number of different substituted 3-quinolinecarboxylic ester derivatives. The preparation of these intermediates could be accomplished by two synthetic routes (Fig. 4): the first (a) is located on C4–C4a and N–C2 in the quinoline ring, and the second (b) involves C3–C4 in conjunction with N–C2.

Through a careful literature search, we found that the second method resulted in overall higher yields, but with more synthetic steps. Theoretically, anthranilic acids could be treated with phosgene to afford corresponding isatoic anhydride. This, after a first *N*-alkylation with iodoalkanes, could then be condensed with diethyl malonate (DEM) or ethyl malonil chloride (EMC) to give the desired ester. Unfortunately, none of the required anthranilic acids were commercially available, but they had to be prepared by using known or modified methods, thus involving too much reaction steps.

Route (a) in Figure 4 appeared most promising. In fact, all substituted esters could be directly obtained by treating the appropriate *para*-substituted anilines with polyesters such as triethyl methanetricarboxylate (TMT), which in turn could be obtained from the diester intermediate. The key step in this scheme was the preparation of the appropriate *para*-substituted anilines as described below.

The acids **2a**, **c**, and **e**–**g** were obtained from respective esters **3a**, **c**, and **e**–**g** in various yields (30–86%) by hydrolysis with HCl (2.8 M) in acetic acid (Scheme 1). The latter were prepared by heating the appropriate *N*-alkylaniline **4a**, **c**, and **e**–**g** with triethyl methanetricarboxylate in Dowtherm A at 220 °C. Unfortunately, the esters **3b**, **d**, and **h** could not be obtained by using this synthetic route. It seems that the *N*-substitution strongly influences the initial coupling and the consequent cyclization reaction to generate the quinoline ring. In particular, starting from the isopropylaniline **4b**, only diester intermediate **5b** was obtained (Scheme 1).

All acids and esters were observed in their enolic form on the 4th-position by NMR and, for compound **2c**, by X-ray crystallography. In particular, signals in the δ 14–14.5 region, which established NOE correlation between the hydroxyl hydrogen in four position and the C_5–*H*, were confirmed by ^{1}H NMR and NOE-difference (Scheme 1).

Only the *N*-alkylaniline **4a** was commercially available; the *para*-benzyl-*N*-alkylanilines **4c**–**e**, **g**, and **h** were synthesized as previously described,[43] by using 1-hydroxymethylbenzotriazole **7** (HMBT) as a synthetic auxiliary (Scheme 2). In fact, **4c**–**e**, **g**, and **h** were obtained in various yields (21–64%) by reacting the appropriate anilines **8c**, **d**, **g**, and **h** with HMBT in acetic acid in the presence of sulfuric acid under reflux, to give **6c**, **d**, **g**, and **h**. Displacement of the benzotriazole group with the appropriate Grignard reagents provided the formation of **4c**–**e**, **g**, and **h** (Scheme 2).

Compounds **8c** and **8d** were commercially available. The synthons **8g** and **8h** were prepared by alkylation of the aniline **12** with the appropriate alkyliodide **9g**, **h** in methanol under reflux, in the presence of a catalytic amount of triethylamine (Scheme 3). It is noteworthy that a small amount of the *N*,*N*-dialkylated products (**13g**, **h**) was isolated.

In the same way, *N*-alkylanilines **4b**, **f** were prepared as above by monoalkylation of the commercially available anilines **10b**, **f** with the appropriate alkyliodide **9b**, **f** (Scheme 4). Also, traces of the dialkylated product **11f** were recovered.

2.3. X-ray crystallography

To study the pharmacophoric features of the 4-hydroxy-2-oxo-1,2-dihydroquinoline-3-carboxylic acid system, the structure of model compound **2c** was determined by X-ray crystallography. Figures 5 and 6 and Table 1 report the structural details of **2c**.

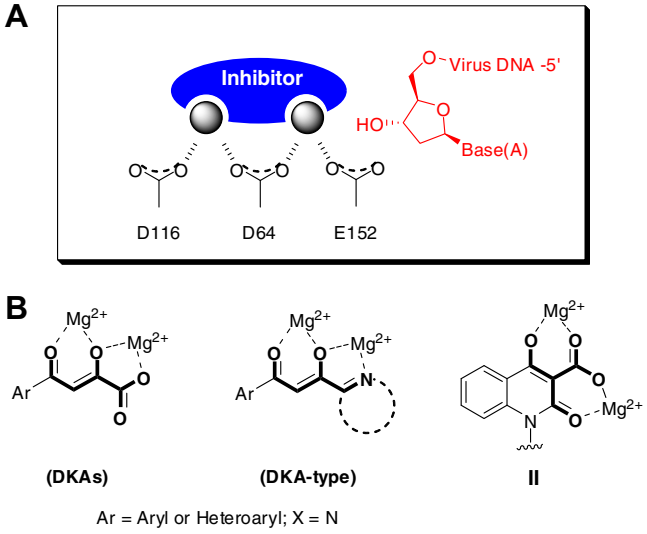

Figure 3. (A) Proposed chelating mechanism for β-diketoacids in the active site of HIV-1 integrase: an inhibitor chelates the two metal ions blocking the host DNA binding. (From Kawasuji et al.).[42] (B) Complexing motif for β-diketoacid, the general scheme of the two metal chelating state for diketoacid-type compounds, and the possible complexing motif for scaffold **II**.

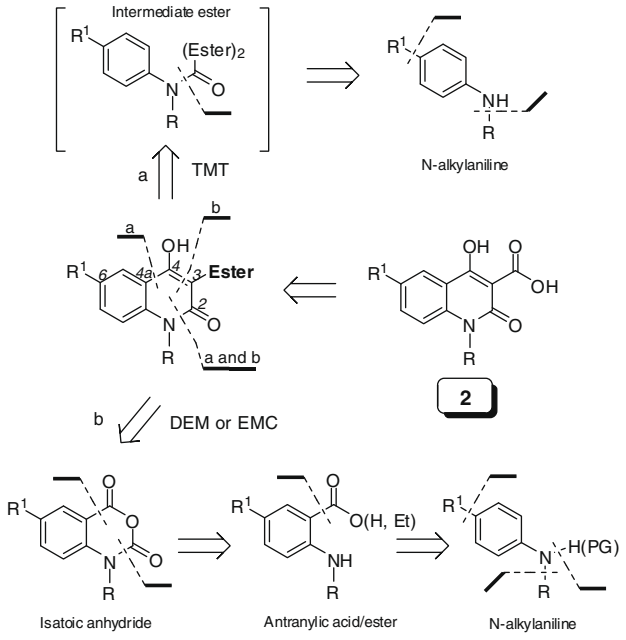

Figure 4. Retrosynthetic plan.

Two independent molecules (Fig. 5) constitute the asymmetric unit of the crystal structure of **2c**. They differ remarkably in the orientation of the benzylic substituent, as shown by the values of the torsion angles around the C4–C7 and C7–C8 bonds that effectively constitute the only conformational degrees of freedom of this otherwise relatively rigid molecule [(C5–C4–C7–C8 = −12.45(1)° and 61.20(1)°; C4–C7–C8–C13 = 95.55(1)° and 45.12(1)°, respectively for the two molecules)]. Both molecules present two strong intramolecular H-bonds involving all the potential donors and acceptors: O2–H...O1 [(D...A = 2.535(5), 2.495(5) Å, D–H...A = 154(3), and 148(5)°, respectively for the two molecules) and O4–H...O3 (D...A = 2.498(5), 2.527(5) Å, D–H...A = 148(5), and 150(5)°, respectively)]. They force both carboxylic groups in the exo configuration. Due to the rigidity and planarity of the aromatic core and to the complete intramolecular H-bond capability, the crystal packing of **2c** is an example of an optimized self-fit molecular shape. This is achieved by placing in close contact a pair of independent molecules not related by any crystallographic symmetry operation.[44] The aromatic cores of the two independent molecules are perfectly parallel within a dihedral angle of 1.60° with an interplanar distance of 3.4 Å (Fig. 5b). Apart from the different conformation of the benzylic arm, the two molecules are approximately related by a rotation around a pseudo twofold axis parallel to the molecular planes (Fig. 5a). Arrays of pseudosymmetric dimers packed by stacking in columns were generated by crystallographic inversions with approximately equal intra- (3.39 Å) and inter-dimer (3.36 Å) separations (Fig. 6).

2.4. Biology

The designed acids **2a**, **c**, and **e**–**g**, and some of the related esters (**3a**, **c**, and **d**) were tested for their ability to inhibit IN catalytic activity in an *in vitro* assay employing purified enzyme as previously described.[45] All the acids showed IN inhibitory activity in nanomolar/micromolar ranges, with selectivity toward the strand transfer process, as evidenced by their selectivity indices (Table 2).

In general, acids **2a**, **c**, and **e**–**g** showed differential IN inhibitory profile, thus confirming that the nature of the N1 and C6 substituents in the quinoline ring significantly influenced the inhibition potency. In particular, compounds **2c**, and **e**–**g** displayed inhibitory activities for strand transfer at IC_{50} values in a range of 0.9–14 μM. An optimal structural combination resulted with the benzyl substituent in C6 of the quinoline ring, eventually bearing a fluorine in *para*-position, and a small alkyl group such as a methyl, located in N1. Comparison between **2c** and **2e** shows the positive influence of the electron withdrawing fluorine atom in the inhibitory activity.

Furthermore, in the 6-F-benzyl derivatives, elongation of the alkyl substituent in the N1 position with a pentyl chain (**2g**), reduced the activity by about 6-fold with respect to the methyl homologue **2e** (IC_{50} = 5 ± 2 versus 0.9 ± 0.4 μM for strand transfer for **2g** and **2e**, respectively). Derivative **2f**, containing an oxy-phenyl substituent at C6, was less potent (IC_{50} = 14 ± 2 μM and 34 ± 8 μM, for strand transfer and 3′-processing, respectively) than **1**. This indicates that, although a bioisosteric substitution of the benzylic methylene with an oxygen seems not to be so different, the size and shape of the oxo-phenyl moiety play, together with the hydrophobic benzyl substituent, an important role in the IN inhibitory activity of this set of compounds.

Compound **2e** proved to be the most potent compound tested, with an inhibition profile and a selectivity index (SI = 26 and 28, for **2e** and L-731,988, respectively) similar to the reference compound L-731,988 (IC_{50} = 0.54 ± 0.08 μM for strand transfer), and therefore it can constitute a promising candidate for further optimization. Further, mapping of the quinolone 3-carboxylic acid pharmacophore onto compounds **2e** and **2g** shows a good agreement between features of the pharmacophore and chemical features of the compounds (Fig. 7). As anticipated, the acids **2c**, **e**, and **g** were more active than the quinoline carboxamide lead compound **1a** (IC_{50s} = 9 ± 5 and 9 ± 4 μM for strand transfer and 3′-processing, respectively). The bioisosteric replacement of the amide functionality with the carboxylic acid group provided a suitable strategy in lead modification for IN inhibition.

The esters **3a** and **3e** are inactive and **3c** had a very low activity (IC_{50} = 110 ± 21 μM for strand transfer). Replacement of the carboxylic acid group with an ester dramatically leads to a loss in IN inhibitory activity, and this underscores the importance of a free carboxylic group on the pharmacophoric fragment, as already observed for the diketo acid class of IN inhibitors.

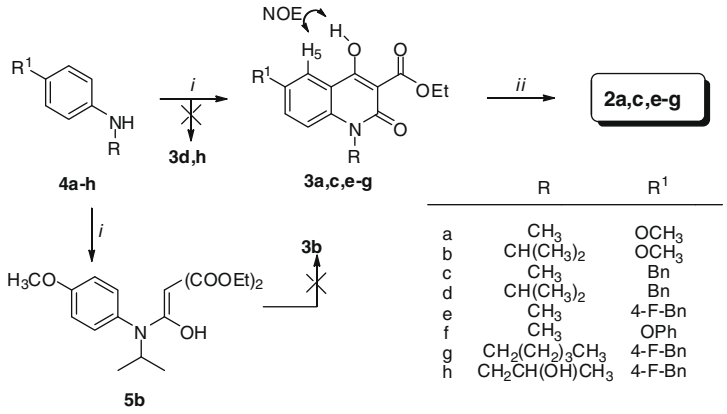

Scheme 1. Preparation of **2a**, **c**, **e**–**g** and of their esters **3a**, **c**, **e**–**g**. Reagents and conditions: (i) $CH(COOCH_2CH_3)_3$, Dowtherm A, 220 °C, 4 h; (ii) 2.8 M HCl in CH_3COOH, 60 °C, 6 h.

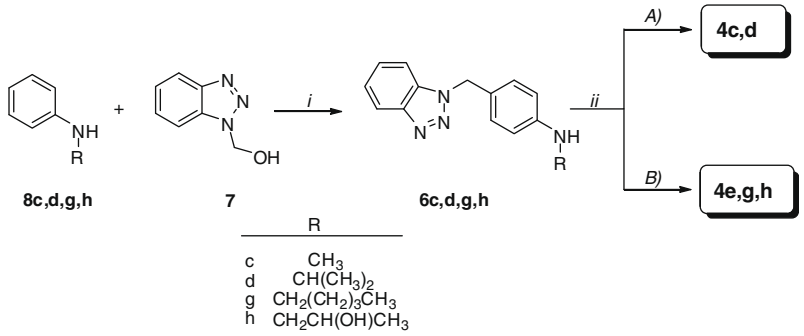

Scheme 2. Preparation of intermediates **4c**–**e**, **g**, **h**. Reagents and conditions: (i) Conc. H_2SO_4, CH_3COOH, reflux, 2 h; ii) A: 2M PhMgBr in Et_2O, toluene, reflux, 12 h; B: 3M 4-F-PhMgBr in Et_2O, toluene, reflux, 12 h.

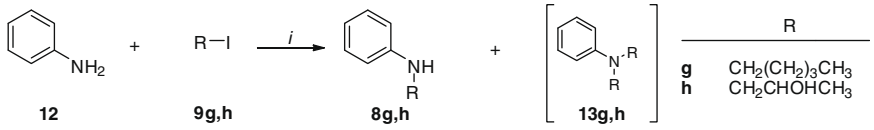

Scheme 3. Preparation of intermediates **8g**, **h**. Reagents and conditions: (i) Triethylamine, CH_3OH, reflux, 3 h.

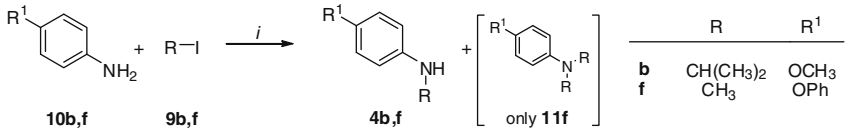

Scheme 4. Preparation of intermediates **4b**, **f**. Reagents and conditions: (i) Triethylamine, CH_3OH, reflux, 3 h.

All compounds were also tested for their cytotoxicity against two colon cancer cell lines (HCT116 p53+/+ and HCT116 p53−/−, Table 2). None of the compounds showed cytotoxicity (CC_{50} > 10 μM) at concentration values about 2.5–15-fold higher than their enzymatic inhibition activity values.

In conclusion, the bioisosteric replacement of the amide in the compound **1a** with a carboxylate group in the scaffold **II** resulted in the discovery of a series of potent IN inhibitors. Similar to previously reported diketo acid IN inhibitors, these compounds are expected to chelate metal ions in the active site of IN. Further derivatization of the scaffold **II** gave compounds that can be mapped by the quinolone 3-carboxylic acid pharmacophore. These promising results warrant further optimization studies on some of the potent compounds.

3. Experimental

3.1. General procedures chemistry

Anhydrous solvents and all reagents were purchased from Aldrich, Merck or Carlo Erba. All reactions involving air- or moisture-sensitive compounds were performed under nitrogen atmosphere using oven-dried glassware and syringes to transfer solutions. Melting points (mp) were determined using an Electro-

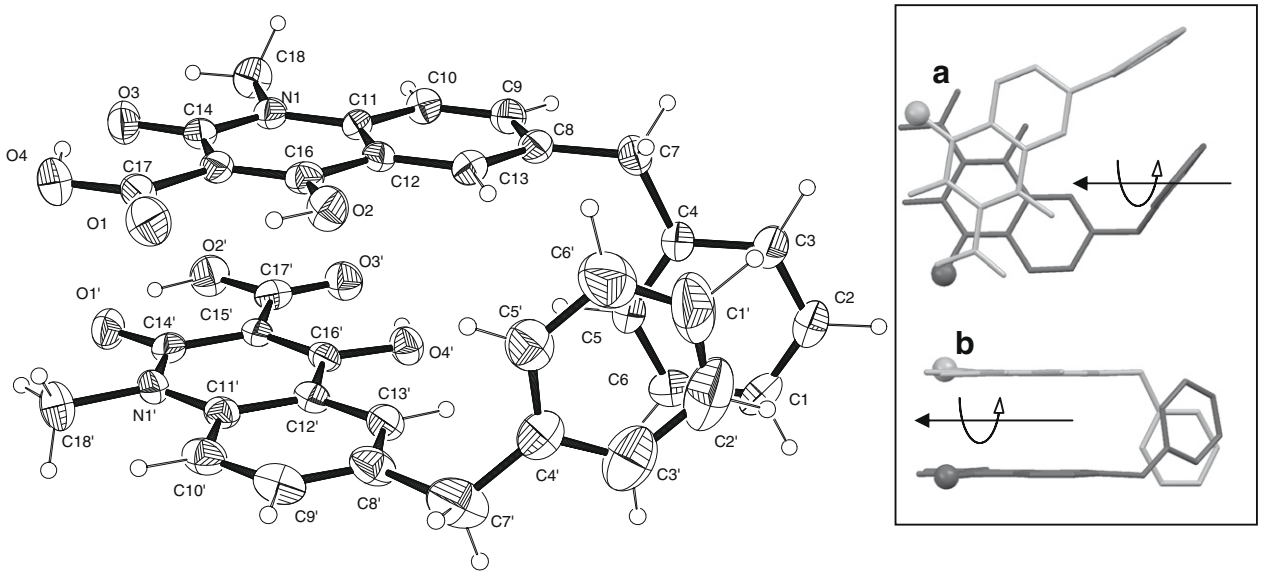

Figure 5. Perspective view and labeling of the two independent molecules in the crystal structure of **2c**. Thermal ellipsoid at the 30% probability level. Inset: top (a) and edge-on (b) views of the pseudosymmetric dimer showing a pseudo two fold axis (hydrogens omitted and methyls C18 shown as balls).

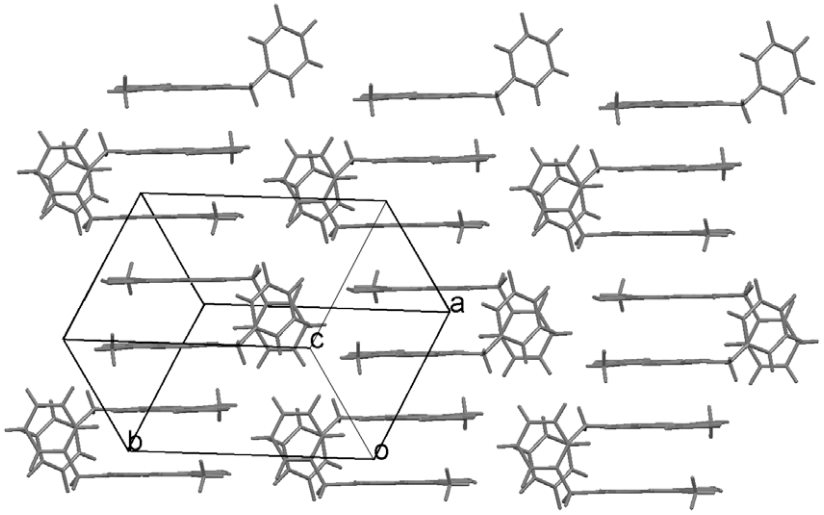

Figure 6. Column stacking of the asymmetric dimers in the crystal packing of **2c**.

thermal or a Köfler apparatus and are uncorrected. Infrared (IR) spectra were recorded in nujol with a Perkin-Elmer 781 IR spectrophotometer and are expressed in ν (cm^{-1}). Nuclear magnetic resonance (^1H NMR and NOE-difference) spectra were determined in $CDCl_3$ and DMSO-d_6 on a Varian XL-200 (200 MHz) spectrometer. Chemical shifts (δ scale) are reported in parts per million (ppm) downfield from tetramethylsilane (TMS) used as an internal standard. The assignment of exchangeable protons (O*H* and N*H*) was confirmed by the addition of D_2O. Electron ionization mass spectra (70 eV) were recorded on a Hewlett-Packard 5989 Mass Engine Spectrometer. Analytical thin-layer chromatography (TLC) was performed on Merck silica gel F-254 plates. For flash chromatography Merck Silica gel 60 was used with a particle size 0.040–0.063 mm (230–400 mesh ASTM). Elemental analyses were performed on a Perkin-Elmer 2400 instrument at Laboratorio di Microanalisi, Dipartimento di Chimica, Università di Sassari (Italy), all values are given as percentages, and the results were within ±0.4% of the theoretical values.

3.1.1. General method for the preparation of 1-R^1-6-R^2-4-hydroxy-2-oxo-1,2 dihydroquinoline-3-carboxylic acids (2a, c, e–g)

To a solution of acetic anhydride (450 mL) at 0 °C was slowly added (caution, exothermic reaction!) concentrated HCl (138 mL, 37%), (76.5% of acetic anhydride and 23.5% of 37% HCl). This yields an approximately 2.8 M solution of HCl in acetic acid with a low water content. To the appropriate ester **3a**, **c**, **e–g** (1.08 mmol of **3a**; 0.593 mmol of **3c**; 0.579 mmol of **3e**; 0.206 mmol of **3f**; 0.607 mmol of **3g**) was added an appropriate amount of the above solution (3 mL per **2a**; 2 mL per **2c** e **2e**; 0.60 mL per **2f**; 1.75 mL per **2g**) of 2.8 M HCl in acetic acid, and the mixture was first heated at 60 °C and then refluxed for 4 h.

Table 1
Crystal data and structure refinement for **2c**.

Empirical formula	$C_{18}H_{15}NO_4$
Formula weight	309.31
Temperature (K)	293(2)
Wavelenght (Å)	1.54184
Crystal system	Triclinic
Space group	$P\bar{1}$
Unit cell dimensions (Å, °)	$a = 13.3745(6)$, $\alpha = 70.651(4)$ $b = 12.8379(6)$, $\beta = 109.248(4)$ $c = 9.9181(3)$, $\gamma = 104.759(5)$
Volume (Å^3)	1496.6(1)
Z	4
Density (calculated) (Mg/m^3)	1.373
Absorption coefficient (mm^{-1})	0.806
$F(000)$	648
Theta range for data collection	3.5–70.0
Reflections collected	5682
Independent reflections	5682
Refinement method	Full-matrix least-squares on F^2
Data/restraints/parameters	5682/0/493
Goodness-of-fit on F^2	0.790
Final R indices [$I > 2\sigma(I)$]	$R_1 = 0.0535$, $wR_2 = 0.0952$
R indices (all data)	$R_1 = 0.1963$, $wR_2 = 0.1383$
Final ΔF maximum/minimum (e Å^{-3})	0.225/−0.188

After the mixture was cooled to room temperature and diluted with 2-propanol, the crystals were filtered off, washed with 2-propanol, and dried in a vacuum to furnish the title compounds as a white-beige solid.

3.1.1.1. 4-Hydroxy-6-methoxy-1-methyl-2-oxo-1,2-dihydroquinoline-3-carboxylic acid (2a). Yield 85%; mp 260–262 °C. IR (nujol) ν cm^{-1} 1671 (C=O acid), 1604 (C=O amide). ^{1}H NMR (DMSO-d_6) δ 16.36 (bs, 1H, COOH), 14.41 (bs, 1H, OH), 8.30 (s, 1H, Ar-H), 7.73 (d, 1H, Ar-H), 7.53 (d, 1H, Ar-H), 3.89 (s, 3H, NCH_3), 3.73 (s, 3H, OCH_3). MS: m/z 249 (M^+). Anal. Calcd. for $C_{12}H_{11}NO_5$: C, 57.83; H, 4.45; N, 5.62. Found: C, 57.60; H, 4.18; N, 5.78.

3.1.1.2. 6-Benzyl-4-hydroxy-1-methyl-2-oxo-1,2-dihydroquinoline-3-carboxylic acid (2c). Yield 30%; mp 158–159 °C. IR (nujol) ν cm^{-1} 1685 (C=O acid), 1627 (C=O amide). ^{1}H NMR ($CDCl_3$) δ 15.65 (bs, 1H, COOH), 14.53 (bs, 1H, OH), 8.09 (s, 1H, Ar-H), 7.61 (d, 1H, Ar-H), 7.41–7.04 (m, 6H, Ar-H), 4.11 (s, 2H, $PhCH_2$), 3.73 (s, 3H, NCH_3). MS m/z 309 (M^+). Anal. Calcd. for $C_{18}H_{15}NO_4$: C, 69.88; H, 4.89; N, 4.53. Found: C, 69.66; H, 4.65; N, 4.87.

3.1.1.3. 6-(4-Fluorobenzyl)-4-hydroxy-1-methyl-2-oxo-1,2-dihydroquinoline-3-carboxylic acid (2e). Yield 47%; mp 165–166 °C. IR (nujol) ν cm^{-1} 1680 (C=O acid), 1598 (C=O amide). ^{1}H NMR ($CDCl_3$) δ 15.63 (bs, 1H, COOH), 14.56 (bs, 1H, OH), 8.07 (s, 1H, Ar-H), 7.58 (d, 1H, Ar-H), 7.45–6.90 (m, 5H, Ar-H), 4.08 (s, 2H, $PhCH_2$), 3.74 (s, 3H, NCH_3). MS m/z 327 (M^+). Anal. Calcd. for $C_{18}H_{14}FNO_4$: C, 66.04; H, 4.31; N, 4.28. Found: C, 66.36; H, 4.16; N, 4.56.

3.1.1.4. 4-Hydroxy-1-methyl-2-oxo-6-phenoxy-1,2-dihydroquinoline-3-carboxylic acid (2f). Yield 66%; mp 193–195 °C. IR (nujol) ν cm^{-1} 1678 (C=O acid), 1620 (C=O amide). ^{1}H NMR ($CDCl_3$) δ 15.6 (s, 1H, COOH), 14.51 (s, 1H, OH), 7.78 (s, 1H, Ar-H), 7.52–6.95 (m, 7H, Ar-H), 3.77 (s, 3H, NCH_3). MS m/z 311 (M^+). Anal. Calcd. for $C_{17}H_{13}NO_5$: C, 65.58; H, 4.21; N, 4.50. Found: C, 65.76; H, 3.94; N, 4.75.

Table 2
Inhibition of HIV-1 integrase catalytic activities and cytotoxicity of title compounds **2a**, **c**, **e**–**g** and intermediates **3a**, **c**, **e**.

Compound	HIV-1 integrase inhibition IC_{50} (μM)[b]		SI[c]	HCT116 p53+/+ CC_{50} (μM)[d]	HCT116 p53−/− CC_{50} (μM)
	3′-Processing	Strand transfer			
1a[a]	9 ± 5	9 ± 4	1	>10	>10
2a	580	320	1.7	>10	>10
2c	45 ± 15	6 ± 2	7.5	>10	>10
2e	23 ± 7	0.9 ± 0.4	26	>10	>10
2f	34 ± 8	14 ± 2	2.4	>10	>10
2g	92 ± 13	5 ± 2	18.4	>10	>10
3a	>1000	>1000	–	>10	>10
3c	275 ± 23	110 ± 21	2.5	>10	>10
3e	800	220 ± 42	3.6	>10	>10
L-731,988[a]	15 ± 2	0.54 ± 0.08	28	>10	>10

[a] Reference compounds: from Dayam et al.[33] (**1a**) and from Sechi et al.[36] (L-731,988).
[b] IC_{50}, inhibitory concentration 50% (average data for inhibition of 3′-processing and strand transfer of purified IN).
[c] SI, selectivity index.
[d] CC_{50}, cytotoxic concentration 50%.

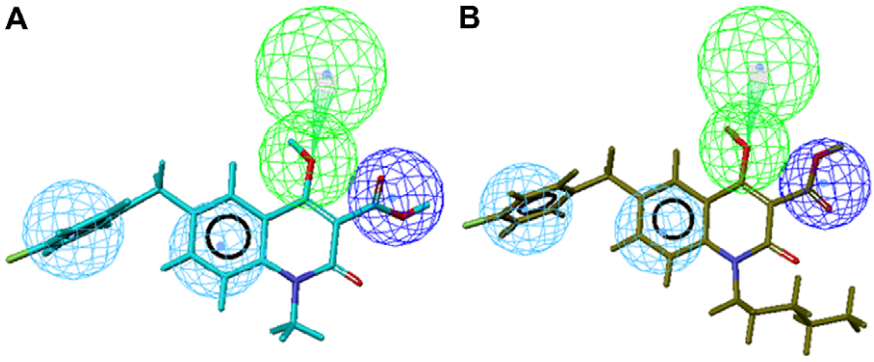

Figure 7. Compounds **2e** (A) and **2g** (B) are mapped onto the quinolone 3-carboxylic acid pharmacophore.

3.1.1.5. 6-(4-Fluorobenzyl)-4-hydroxy-2-oxo-1-pentyl-1,2-dihydroquinoline-3-carboxylic acid (2g). Yield 43%; mp 140–142 °C. IR (nujol) ν cm^{-1}1680 (C=O acid), 1610 (C=O amide). ^{1}H NMR ($CDCl_3$) δ 15.78 (bs, 1H, COOH), 14.54 (bs, 1H, OH), 8.09 (s, 1H, Ar-H), 7.57 (d, 1H, Ar-H), 7.40–6.91 (m, 5H, Ar-H), 4.28 (s, 2H, NCH_2), 4.08 (s, 2H, $PhCH_2$), 1.86–1.27 (m, 6H, CH_2), 0.93 (t, 3H, CH_3). MS m/z 383 (M^+). Anal. Calcd. for $C_{22}H_{22}FNO_4$: C, 68.90; H, 5.79; N, 3.65. Found: C, 69.22; H, 5.45; N, 3.87.

3.1.2. General method for the preparation of 1-R^1-6-R^2-4-hydroxy-2-oxo-1,2-dihydroquinoline-3-carboxylic esters (3a, c, e–g)

To solution of the appropriate alkylamine **4a**, **c**, **e**–**g** (1 equiv; 0.5 g, 3.65 mmol of **4a**; 0.7 g, 3.55 mmol of **4c**; 0.7 g, 3.25 mmol of **4e**; 0.35 g, 1.76 mmol of **4f**; 0.7 g, 2.45 mmol of **4g**) in Dowtherm A (eutectic mixture of diphenyl and diphenyl oxide, 5 mL for **3a**–**h**), methanetricarboxylic acid triethyl ester (3.2 equiv under a nitrogen atmosphere at 180 °C was added). The temperature was slowly raised to 220–225 °C while the formed ethanol was distilled off. The solution was heated for 4 h and then cooled. Ethyl ether and petroleum ether were added and the formed crystalline precipitate was filtered off, washed with ethyl ether and petroleum ether, and dried to afford the desired compound as a white-yellow solid (**3a**, **c**, **e**, **f**) or oil (**3g**).

3.1.2.1. Ethyl 4-hydroxy-6-methoxy-1-methyl-2-oxo-1,2-dihydroquinoline-3-carboxylate (3a). Yield 41%; mp 127–129 °C. IR (nujol) ν cm^{-1} 1639 (ester and amide). ^{1}H NMR ($CDCl_3$) δ 14.22 (s, 1H, OH), 7.57 (s, 1H, Ar-H), 7.29–7.16 (m, 2H, Ar-H), 4.51 (q, 2H, CH_2), 3.89 (s, 3H, NCH_3), 3.64 (s, 3H, OCH_3), 1.49 (t, 3H, CH_3). MS m/z 277 (M^+). Anal. Calcd. for $C_{14}H_{15}NO$: C, 78.83; H, 7.09; N, 6.57. Found: C, 79.20; H, 6.65; N, 6.80.

3.1.2.2. Ethyl 6-benzyl-4-hydroxy-1-methyl-2-oxo-1,2-dihydroquinoline-3-carboxylate (3c). Yield 20%; mp 104–107 °C. IR (nujol) ν cm^{-1} 1667 (ester), 1591 (amide). ^{1}H NMR ($CDCl_3$) δ 14.19 (s, 1H, OH), 8.02 (s, 1H, Ar-H), 7.56–7.04 (m, 7H, Ar-H), 4.28 (q, 2H, $COOCH_2$), 4.63 (s, 2H, CH_2), 3.63 (s, 3H, NCH_3), 1.48 (t, 3H, CH_3). MS: m/z 337 (M^+). Anal. Calcd. for $C_{20}H_{19}NO_4$: C, 71.19; H, 5.68; N, 4.15. Found: C, 71.40; H, 5.40; N, 4.30.

3.1.2.3. Ethyl 6-(4-fluorobenzyl)-4-hydroxy-1-methyl-2-oxo-1,2-dihydroquinoline-3-carboxylate (3e). Yield 20%; mp 161–162 °C. IR (nujol) ν cm^{-1} 1673 (ester), 1600 (amide). ^{1}H NMR ($CDCl_3$) δ 14.20 (s, 1H, OH), 8.00 (s, 1H, Ar-H), 7.56–6.96 (m, 6H, Ar-H), 4.50 (q, 2H, $COOCH_2$), 4.03 (s, 2H, CH_2), 3.63 (s, 3H, NCH_3), 1.48 (t, 3H, CH_3). MS: m/z 355 (M^+). Anal. Calcd. for $C_{20}H_{18}FNO_4$: C, 67.58; H, 5.11; N, 3.94. Found: C, 67.80; H, 4.80; N, 4.20.

3.1.2.4. Ethyl 4-hydroxy-1-methyl-2-oxo-6-phenoxy-1,2-dihydroquinoline-3-carboxylate (3f). Yield 15%; mp 155–158 °C. IR (nujol) ν cm^{-1} 1670 (ester), 1585 (amide). ^{1}H NMR ($CDCl_3$) δ 14.15 (s, 1H, OH), 7.76 (s, 1H, Ar-H), 7.47–6.95 (m, 7H, Ar-H), 4.50 (q, 2H, $COOCH_2$), 3.67 (s, 3H, NCH_3), 1.48 (t, 3H, CH_3). MS m/z 339 (M^+). Anal. Calcd. for $C_{19}H_{17}NO_5$: C, 67.23; H, 5.05; N, 4.13. Found: C, 67.53; H, 4.76; N, 4.45.

3.1.2.5. Ethyl 6-(4-fluorobenzyl)-4-hydroxy-1-pentyl-2-oxo-1,2-dihydroquinoline-3-carboxylate (3g). Yield 38%; oil. IR (nujol) ν cm^{-1} 1661 (ester), 1570 (amide). ^{1}H NMR ($CDCl_3$) δ 14.23 (s, 1H, OH), 8.00 (s, 1H, Ar-H), 7.52–6.88 (m, 6H, Ar-H), 4.50 (q, 2H, $COOCH_2$), 4.26 (s, 2H, CH_2), 4.22 (t, 2H, NCH_2), 4.02 (s, 2H, $PhCH_2$), 1.76–1.60 (m, 2H, NCH_2CH_2), 1.48 (t, 3H, CH_3), 1.59–1.16 (m, 4H, CH_2), 0.91 (t, 3H, CH_3). MS m/z 411 (M^+). Anal. Calcd. for $C_{24}H_{26}FNO_4$: C, 70.04; H, 6.37; N, 3.41. Found: C, 70.30; H, 6.54; N, 3.24.

3.1.3. Preparation of diethyl {hydroxy[(4-methoxyphenyl)(propan-2-yl)amino]methylidene}propanedioate (5b)

To solution of *N*-isopropyl-4-methoxyaniline **4b** (1 equiv; 0.7 g, 4.24 mmol) in Dowtherm A (5 mL) was added methanetricarboxylic acid triethyl ester (3.2 equiv, 2.84 mL) under a nitrogen atmosphere at 180 °C. The temperature was slowly raised to 220–225 °C and the solution was heated for 5 h and then cooled at room temperature. Next, the solution was extracted with 10% NaOH, and the aqueous phase was acidified with 3N HCl. The latter was then extracted with ethyl ether and the organic layer dried over Na_2SO_4. After evaporation of the organic solvent, the crude product was purified by flash chromatography (eluents: petroleum ether–ethyl acetate 8:2) to give an orange oil.

Yield 14%; oil. ^{1}H NMR ($CDCl_3$) δ 14.22 (s, 1H, OH), 7.08–4.82 (dd, 4H, Ar-H), 5.08–4.87 (m, 1H, CH), 4.25 (q, 4H, $2COOCH_2$), 3.83 (s, 3H, OCH_3), 1.24 (t, 6H, $2CH_3$), 1.06 (d,1.07, 6H, CH_3). MS m/z 351 (M^+).

3.1.4. General method for the preparation of 4-(4-R-benzyl)-*N*-alkylanilines (4c–e, g, h)

A solution of the appropriate adduct **6c**–**e**, **g**, **h** (1 equiv; 2.5 g, 9.4 mmol of **6d**; 2 g, 8.39 mmol of **6c**; 3 g, 12 mmol of **6e**; 4 g, 13 mmol of **6g**; 1.5 g, 5.31 mmol of **6h**) in toluene (55 mL for **4d**; 50 mL for **4c**; 75 mL for **4e**; 80 mL for **4g**; 30 mL for **4h**) under nitrogen was added the appropriate Grignard reagent solution (2 M phenylmagnesium bromide in ethyl ether for **4c** and **4d**; 3 M 4-F-phenylmagnesium bromide in ethyl ether for **4e**, **4g** and **4h**) (4 equiv). Next, the reaction mixture was heated at 100 °C for 12 h (monitored by TLC until the starting material had been consumed).

The reaction was cooled, poured into ice-water (200 mL) and acidified with 3N HCl. The resulting solution was made alkaline (pH ~9) with 10% NaOH, and then extracted with ethyl ether. The organic layer was washed with water and dried over Na_2SO_4. After evaporation of the organic solvent, the crude product was purified by flash chromatography (eluents: petroleum ether-ethyl acetate 7:3) to give an orange oil.

3.1.4.1. 4-Benzyl-*N*-methylaniline (4c). Yield 49%; oil. ^{1}H NMR ($CDCl_3$) δ 7.29–7.09 (m, 5H, Ar-H), 7.01 (d, 2H, Ar-H), 6.55 (d, 2H, Ar-H), 3.87 (s, 2H, CH_2), 2.79 (s, 3H, CH_3). MS m/z 197 (M^+).

3.1.4.2. 4-Benzyl-*N*-(propan-2-yl)aniline (4d). Yield 21%; oil. ^{1}H NMR ($CDCl_3$) δ 7.31–7.11 (m, 5H, Ar-H), 7.04–6.91 (m, 2H, Ar-H), 6.60–6.47 (m, 2H, Ar-H), 3.87 (s, 2H, CH_2), 3.67–3.51 (m, 1H, CH), 1.19 (d, 6H, CH_3). MS m/z 225 (M^+).

3.1.4.3. 4-(4-Fluorobenzyl)-*N*-methylaniline (4e). Yield 25%; oil. ^{1}H NMR ($CDCl_3$) δ 7.69–6.83 (m, 8H, Ar-H), 3.84 (s, 2H, CH_2), 2.81 (s, 3H, CH_3). MS m/z 215 (M^+).

3.1.4.4. 4-(4-Fluorobenzyl)-*N*-pentylaniline (4g). Yield 51%; oil. ^{1}H NMR ($CDCl_3$) δ 7.06–6.85 (m, 4H, Ar-H), 6.71–6.48 (m, 4H, Ar-H), 4.37 (s, 2H, CH_2), 3.29 (bs, 1H, NH), 3.07 (t, 2H, CH_2N), 1.75–1.48 (m, 2H, CH_2), 1.43–1.25 (m, 4H, CH_2), 0.89 (d, 3H, CH_3). MS m/z 271 (M^+).

3.1.4.5. 1-{[4-(4-Fluorobenzyl)phenyl]amino}propan-2-ol (4h). Yield 64%; oil. ^{1}H NMR ($CDCl_3$) δ 7.26–6.86 (m, 8H, Ar-H), 4.07–3.95 (m, 1H, CH), 3.84 (s, 2H, CH_2), 3.23 (dd, 1H, CH_2), 2.84 (dd, 1H, CH_2), 1.28 (d, 3H, CH_3). MS m/z 259 (M^+).

3.1.5. General method for the preparation of 4-(1*H*-Benzotriazol-1-ylmethyl)-*N*-alkylaniline (6c, d, g, h)

To a solution of the appropriate *N*-alkylaniline **8c**–**e**, **g**, **h** (1 equiv; 5 g, 0.0467 mol of **8c**, **e**; 2.5 g, 0.018 mol of **8d**; 5 g,

0.030 mol of **8g**; 2.3 g, 0.0152 mol of **8h**) in concentrated sulfuric acid (3.25 mL for **6c**, **e**; 1.65 mL for **6d**; 2 mL for **6g**; 1.05 mL for **6h**) and acetic acid (23 mL for **6c**, **e**; 11 mL for **6d**; 15 mL for **6g**; 8 mL for **6h**) was added 1-hydroxymethyl-(1*H*)-benzotriazole **7** (1 equiv) at 0–10 °C. Next, the mixture was heated for 2 h at 60 °C. Then, the solution was poured into ice-water (200 mL) and neutralized with 10% NaOH 10%. The sticky solid that formed was extracted with ethyl acetate, the organic phases washed with water, and dried over Na_2SO_4. After evaporation of the organic solvent, the crude product was purified by flash chromatography (eluents: petroleum ether-ethyl acetate 8:2) to give an yellow-orange solid or oil.

3.1.5.1. 4-(1H-Benzotriazol-1-ylmethyl)-*N*-methylaniline (6c). Yield 54%; mp 50 °C. ^{1}H NMR ($CDCl_3$) δ 8.04 (d, 1H, Ar-H), 7.46–7.20 (m, 3H, Ar-H), 7.15 (d, 2H, Ar-H), 5.72 (s, 2H, CH_2), 2.78 (s, 3H, CH_3). MS *m*/*z* 238 (M^+).

3.1.5.2. 4-(1H-Benzotriazol-1-ylmethyl)-*N*-(propan-2-yl)aniline (6d). Yield 63%; mp 52 °C. ^{1}H NMR ($CDCl_3$) δ 8.04 (d, 1H, Ar-H), 7.47–7.25 (m, 3H, Ar-H), 7.14 (d, 2H, Ar-H), 6.52 (d, 2H, Ar-H), 5.71 (s, 2H, CH_2), 3.67–3.42 (m, 1H, CH), 1.18 (d, 6H, CH_3). MS *m*/*z* 266 (M^+).

3.1.5.3. 4-(1H-benzotriazol-1-ylmethyl)-*N*-pentylaniline (6g). Yield 27%; oil. ^{1}H NMR ($CDCl_3$) δ 8.04 (d, 1H, Ar-H), 7.43–7.24 (m, 3H, Ar-H), 7.14 (d, 2H, Ar-H), 6.53 (d, 2H, Ar-H), 5.72 (s, 2H, CH_2), 3.61 (t, 2H, CH_2N), 1.67–1.52 (m, 2H, CH_2), 1.38–1.17 (m, 4H, CH_2), 0.92 (t, 3H, CH_3). MS *m*/*z* 294 (M^+).

3.1.5.4. 1-{[4-(1H-Benzotriazol-1-ylmethyl)phenyl]amino}propan-2-ol (6h). Yield 23%; oil. ^{1}H NMR ($CDCl_3$) δ 8.03 (d, 1H, Ar-H), 7.44–7.24 (m, 3H, Ar-H), 7.14 (d, 2H, Ar-H), 6.56 (d, 2H, Ar-H), 5.70 (s, 2H, CH_2), 5.17–5.00 (m, 1H, CH), 3.29–3.15 (m, 2H, CH_2), 1.28 (d, 3H, CH_3). MS *m*/*z* 282 (M^+).

3.1.6. General method for the preparation of 4-R-*N*-alkylanilines (4b, f, and 8g, h)

A solution with the appropriate 4-R-aniline **10b**, **f** and **12** (1 equiv; 1.5 g, 0.0122 mol of **10b**; 2 g, 0.0108 mol of **10f**; 5 g, 0.0537 mol of **12**), the respective iodoalkane **9b**, **f**, **g**, **h** (1 equiv), and triethylamine (1 equiv) in 15 mL of methanol was heated under reflux for 4 h. Then, the solvent was removed under vacuum and water was added to the crude product. The resulting mixture was extracted with ethyl acetate, and the organic layer was dried over Na_2SO_4. After evaporation of the organic solvent, the product was purified by flash chromatography (eluents: petroleum ether-ethyl acetate 8:2 for **4b**, **f**, and **8g**, **h**; petroleum ether-ethyl acetate 9.5:0.5 for **11f** e **13g**, **h**) to give an yellow-orange oil. In addition to the mono-*N*-alkylation, a small amount of the dialkylated derivatives **11f** and **13g**, **h** were obtained.

3.1.6.1. 4-Methoxy-*N*-(propan-2-yl)aniline (4b). Yield 72%; oil. ^{1}H NMR ($CDCl_3$) δ 6.77 (d, 2H, Ar-H), 6.55 (d, 2H, Ar-H), 3.74 (s, 3H, OCH_3), 3.61–3.46 (m, 1H, CH), 2.04(s, 1H, NH), 1.18 (d, 6H, CH_3). MS *m*/*z* 165 (M^+).

3.1.6.2. N-Pentylaniline (8g). Yield 30%; oil. ^{1}H NMR ($CDCl_3$) δ 7.16 (m, 2H, Ar-H), 6.75–6.53 (m, 3H, Ar-H), 3.5 (bs, 1H, NH), 3.07 (t, 2H, CH_2N), 1.70–1.48 (m, 2H, CH_2), 1.46–1.02 (m, 4H, CH_2), 0.93 (t, 3H, CH_3). MS *m*/*z* 163 (M^+).

3.1.6.3. *N*,*N*-Dipentylaniline (13g). Yield 10%; oil. ^{1}H NMR (200 MHz, $CDCl_3$) δ 7.20 (m, 2H, Ar-H), 6.68–6.53 (m, 3H, Ar-H), 3.24 (t, 4H, CH_2N), 1.66–1.46 (m, 4H, CH_2), 1.44–1.20 (m, 8H, CH_2), 0.90 (t, 6H, CH_3). MS *m*/*z* 223 (M^+).

3.1.6.4. *N*-Methyl-4-phenoxyaniline (4f). Yield 23%; oil. ^{1}H NMR ($CDCl_3$) δ 7.32–7.20 (m, 2H, Ar-H), 7.04–6.80 (m, 3H, Ar-H), 6.65–6.55 (m, 2H, Ar-H), 2.84 (s, 3H, CH_3). MS *m*/*z* 199 (M^+).

3.1.6.5. *N*,*N*-Dimethyl-4-phenoxyaniline (11f). Yield 10%; oil. ^{1}H NMR ($CDCl_3$) δ 7.32–7.20 (m, 2H, Ar-H), 7.04–6.80 (m, 3H, Ar-H), 6.78–6.67 (m, 2H, Ar-H), 2.93 (s, 6H, CH_3). MS *m*/*z* 213 (M^+).

3.1.6.6. 1-(Phenylamino)propan-2-ol (8h). Yield 60%; oil. ^{1}H NMR ($CDCl_3$) δ 7.20–7.02 (m, 2H, Ar-H), 6.74–6.50 (m, 3H, Ar-H), 4.16–4.00 (m, 1H, CH), 3.59 (bs, 1H, NH), 3.02–2.81 (m, 2H, CH_2), 1.21 (d, 3H, CH_3). MS *m*/*z* 151 (M^+).

3.1.6.7. 1,1′-(Phenylamino)dipropan-2-ol (13h). Yield 2.5%; oil. ^{1}H NMR ($CDCl_3$) δ 7.31–7.15 (m, 2H, Ar-H), 6.84–6.52 (m, 3H, Ar-H), 4.24–4.04 (m, 2H, CH), 3.27–2.93 (m, 4H, CH_2), 1.23 (d, 6H, CH_3). MS *m*/*z* 209 (M^+).

3.2. X-ray crystallography

Crystals of **2c** suitable for X-ray diffraction were obtained by slow evaporation from $CHCl_3$. Single crystal X-ray diffraction analysis was carried out at room temperature with a computer-controlled Siemens AED diffractometer using CuKα (λ = 1.54178 Å). No crystal decay was observed. The intensity data were processed with a peak-profile analysis procedure and corrected for Lorentz and polarization effects. The phase problem was solved by direct methods using SIR 2004.[46] Full-matrix least-squares refinements were carried out with SHELXS 97,[47] implemented in the WinGX package.[48] Anisotropic thermal displacement parameters were refined for all non H atoms. H atoms were partly located on Fourier maps and partly introduced in calculated positions, then all were refined isotropically. The Cambridge Crystallographic Database software[49] and PARST97[50] were used for analyzing and drawing the molecular structures. Data concerning structure solution and refinement are presented in Table 1.

Crystallographic data (excluding structure factors) for **2c** have been deposited with the Cambridge Crystallographic Data Centre as supplementary publications nos. CCDC 692283. Copies of the data can be obtained free of charge on application to CCDC, 12 Union Road, Cambridge CB2 1EZ, UK (fax: +44 1223 336 033; e-mail: deposit@ccdc.cam.ac.uk).

3.3. Biology

3.3.1. Materials, chemicals, and enzymes

All compounds were dissolved in DMSO and the stock solutions were stored at –20 °C. The γ [^{32}P]-ATP was purchased from Perkin-Elmer. The expression systems for the wild-type IN was a generous gift from Dr. Robert Craigie, Laboratory of Molecular Biology, NIDDK, NIH, Bethesda, MD.

3.3.2. Preparation of oligonucleotide substrates

The oligonucleotides 19top, 5′-GTGTGGAAAATCTCTAGCA-3′ and 21bot, 5′-ACTGCTAGAGATTTTCCACAC-3′ were purchased from Norris Cancer Center Microsequencing Core Facility (University of Southern California) and purified by UV shadowing on polyacrylamide gel. To analyze the extent of strand transfer using 5′-end labeled substrates, 19top was 5′-end labeled using T_4 polynucleotide kinase (Epicentre, Madison, WI) and γ [^{32}P]-ATP (Amersham Biosciences or ICN). The kinase was heat-inactivated and 21bot was added in 1.5-molar excess. The mixture was heated at 95 °C, allowed to cool slowly to room temperature, and run through a spin 25 mini-column (USA Scientific) to separate annealed double-stranded oligonucleotide from unincorporated material.

3.3.3. Integrase assays

To determine the extent of strand transfer, wild-type IN was preincubated at a final concentration of 200 nM with the inhibitor in reaction buffer (50 mM NaCl, 1 mM HEPES, pH 7.5, 50 μM EDTA, 50 μM dithiothreitol, 10% glycerol (w/v), 7.5 mM $MnCl_2$, 0.1 mg/mL bovine serum albumin, 10 mM 2-mercaptoethanol, 10% dimethyl sulfoxide, and 25 mM MOPS, pH 7.2) at 30 °C for 30 min. Then, 20 nM of the 5′-end ^{32}P-labeled linear oligonucleotide substrate was added, and incubation was continued for an additional 1 h. Reactions were quenched by the addition of an equal volume (16 μL) of loading dye (98% deionized formamide, 10 mM EDTA, 0.025% xylene cyanol and 0.025% bromophenol blue). An aliquot (5 μL) was electrophoresed on a denaturing 20% polyacrylamide gel (0.09 M tris–borate pH 8.3, 2 mM EDTA, 20% acrylamide, 8M urea).

Gels were dried, exposed in a PhosphorImager cassette, and analyzed using a Typhoon 8610 Variable Mode Imager (Amersham Biosciences) and quantitated using ImageQuant 5.2. Percent inhibition (% *I*) was calculated using the following equation:

$$\%I = 100 \times [1 - (D - C)/(N - C)]$$

where *C*, *N*, and *D* are the fractions of 21-mer substrate converted to strand transfer products for DNA alone, DNA plus IN, and IN plus drug, respectively. The IC_{50} values were determined by plotting the logarithm of drug concentration *versus* percent inhibition to obtain concentration that produced 50% inhibition.

3.3.4. Cell culture

The HCT116 P53+/+ and HCT116 P53−/− cells were kindly provided by Dr. Bert Vogelstein (Johns Hopkins Medical Institutions, Baltimore, MD). Cells were maintained as monolayer cultures in RPMI 1640 media supplemented with 10% fetal bovine serum (Gemini-Bioproducts, Woodland, CA) and 2 mmol/L L-glutamine at 37 °C in a humidified atmosphere of 5% CO_2. To remove the adherent cells from the flask for passaging and counting, cells were washed with PBS without calcium or magnesium, incubated with a small volume of 0.25% trypsin–EDTA solution (Sigma–Aldrich, St. Louis, MO) for 5–10 min, and washed with culture medium and centrifuged. All experiments were performed using cells at exponential growth stage. Cells were routinely checked for *mycoplasma* contamination using a PCR-based assay (Stratagene, Cambridge, UK).

3.3.5. Drugs

Stock solutions (10 mM) of compounds were prepared in DMSO and stored at 20 °C. Further dilutions were made fresh in PBS or cell-culture media.

3.3.6. Cytotoxicity assays

Cytotoxicity was assessed by a 3-(4,5-dimethylthiazol-2-yl)-2,5-diphenyltetrazolium bromide (MTT) assay as previously described.[51] Briefly, cells were seeded in 96-well microtiter plates and allowed to attach. Cells were subsequently treated with continuous exposure to the corresponding drug for 72 h. An MTT solution (at a final concentration of 0.5 mg/mL) was added to each well, and cells were incubated for 4 h at 37 °C. After removal of the medium, DMSO was added and the absorbance was read at 570 nm. All assays were done in triplicate. The IC_{50} was then determined for each drug from a plot of log (drug concentration) versus percentage of cells killed.

Acknowledgments

We thank Dr. Maria Orecchioni and Mr. Paolo Fiori for assistance with NMR spectroscopy. M.S. is grateful to Fondazione Banco di Sardegna and to Università di Sassari for their partial financial support. The work in NN's laboratory was supported by funds from the Campbell Foundation. The authors thank the 'Laboratorio di Strutturistica Mario Nardelli' of the University of Parma for facilities.

References and notes

1. Barbaro, G.; Scozzafava, A.; Mastrolorenzo, A.; Supuran, C. T. *Curr. Pharm. Des.* **2005**, *11*, 1843.
2. Cohen, J. *Science* **2002**, *296*, 2320.
3. De Clercq, E. *Nat. Rev. Drug Discov.* **2002**, *1*, 13.
4. Neamati, N.; Marchand, C.; Pommier, Y. *Adv. Pharmacol.* **2000**, *49*, 147.
5. d'Angelo, J.; Mouscadet, J. F.; Desmaele, D.; Zouhiri, F.; Leh, H. *Pathol. Biol.* **2001**, *49*, 237.
6. Neamati, N. *Exp. Opin. Invest. Drugs* **2001**, *10*, 281.
7. Anthony, N. J. *Curr. Top. Med. Chem.* **2004**, *4*, 979.
8. Pommier, Y.; Johnson, A. A.; Marchand, C. *Nat. Rev. Drug Discov.* **2005**, *4*, 236.
9. Brown, P. O. Integration. In *Retroviruses*; Coffin, J. M., Hughes, S. H., Varmus, H. E., Eds.; Cold Spring Harbor Laboratory Press: NY, 1997; pp 161–203.
10. Pais, G. C. G.; Burke, T. R. *Drugs Future* **2002**, *27*, 1101.
11. Kiyama, R.; Kawasuji, T. PCT Int. Appl. **2001**, WO-01/95905.
12. Hazuda, D. J.; Felock, P.; Witmer, M.; Wolfe, A.; Stillmock, K.; Grobler, J. A.; Espeseth, A.; Gabryelski, L.; Schleif, W.; Blau, C.; Miller, M. D. *Science* **2000**, *287*, 646.
13. Goldgur, Y.; Dyda, F.; Hickman, A. B.; Jenkins, T. M.; Craigie, R.; Davies, D. R. *Proc. Natl. Acad. Sci. U.S.A.* **1998**, *95*, 9150.
14. Marchand, C.; Zhang, X.; Pais, G. C. G.; Cowansage, K.; Neamati, N.; Burke, T. R., Jr.; Pommier, Y. *J. Biol. Chem.* **2002**, *277*, 12596.
15. Pais, G. C. G.; Zhang, X.; Marchand, C.; Neamati, N.; Cowansage, K.; Svarovskaia, E. S.; Pathak, V. K.; Tang, Y.; Nicklaus, M.; Pommier, Y.; Burke, T. R., Jr. *J. Med. Chem.* **2002**, *45*, 3184.
16. Pluymers, W.; Pais, G.; Van Maele, B.; Pannecouque, C.; Fikkert, V.; Burke, T. R., Jr.; De Clercq, E.; Witvrouw, M.; Neamati, N.; Debyser, Z. *Antimicrob. Agents Chemother.* **2002**, *46*, 3292.
17. Sechi, M.; Derudas, M.; Dallocchio, R.; Dessi, A.; Bacchi, A.; Sannia, L.; Carta, F.; Palomba, M.; Ragab, O.; Chan, C.; Shoemaker, R.; Sei, S.; Dayam, R.; Neamati, N. *J. Med. Chem.* **2004**, *47*, 5298.
18. Billich, A. *Curr. Opin. Invest. Drugs* **2003**, *4*, 206.
19. Johnson, A. A.; Marchand, C.; Pommier, Y. *Curr. Top. Med. Chem.* **2004**, *4*, 671.
20. Wang, Y.; Serradell, N.; Bolos, J.; Rosa, E. *Drugs Future* **2007**, *32*, 118.
21. Sorbera, L. A.; Serradell, N. *Drugs Future* **2006**, *31*, 310.
22. Nicklaus, M. C.; Neamati, N.; Hong, H.; Mazumder, A.; Sunder, S.; Chen, J.; Milne, G. W.; Pommier, Y. *J. Med. Chem.* **1997**, *40*, 920.
23. Neamati, N.; Hong, H.; Mazumder, A.; Wang, S.; Sunder, S.; Nicklaus, M. C.; Milne, G. W.; Proksa, B.; Pommier, Y. *J. Med. Chem.* **1997**, *40*, 942.
24. Chen, I.-J.; Neamati, N.; MacKerrel, A. D., Jr. *Curr. Drug Target Infect. Dis.* **2002**, *2*, 217.
25. Gupta, S. P.; Nagappa, A. N. *Curr. Med. Chem.* **2003**, *10*, 1779.
26. Maurin, C.; Bailly, F.; Cotelle, P. *Curr. Med. Chem.* **2003**, *10*, 1795.
27. Long, Y. Q.; Jiang, X. H.; Dayam, R.; Sanchez, T.; Shoemaker, R.; Sei, S.; Neamati, N. *J. Med. Chem.* **2004**, *47*, 2561.
28. Barreca, M. L.; Rao, A.; De Luca, L.; Zappala, M.; Gurnari, C.; Monforte, P.; De Clercq, E.; Van Maele, B.; Debyser, Z.; Witvrouw, M.; Briggs, J. M.; Chimirri, A. *J. Chem. Inf. Comput. Sci.* **2004**, *44*, 1450.
29. Dayam, R.; Sanchez, T.; Clement, O.; Shoemaker, R.; Sei, S.; Neamati, N. *J. Med. Chem.* **2005**, *48*, 111.
30. Sechi, M.; Sannia, L.; Carta, F.; Palomba, M.; Dallocchio, R.; Dessì, A.; Derudas, M.; Zawahir, Z.; Neamati, N. *Antiviral Chem. Chemother.* **2005**, *16*, 41.
31. Deng, J.; Lee, K. W.; Sanchez, T.; Cui, M.; Neamati, N.; Briggs, J. M. *J. Med. Chem.* **2005**, *48*, 1496.
32. Dayam, R.; Sanchez, T.; Neamati, N. *J. Med. Chem.* **2005**, *48*, 8009.
33. Dayam, R.; Sanchez, T.; Neamati, N. *ChemMedChem* **2006**, *1*, 238.
34. Dayam, R.; Al-Mawsawi, L. Q.; Zawahir, Z.; Witvrouw, M.; Debyser, Z.; Neamati, N. *J. Med. Chem.* **2008**, *51*, 1136.
35. Maurin, C.; Bailly, F.; Buisine, E.; Vezin, H.; Mbemba, G.; Mouscadet, J. F.; Cotelle, P. *J. Med. Chem.* **2004**, *47*, 5583.
36. Sechi, M.; Bacchi, A.; Carcelli, M.; Compari, C.; Duce, E.; Fisicaro, E.; Rogolino, D.; Gates, P.; Derudas, M.; Al-Mawsawi, L. Q.; Neamati, N. *J. Med. Chem.* **2006**, *49*, 4248.
37. Sotriffer, C. A.; Ni, H.; McCammon, A. J. *J. Am. Chem. Soc.* **2000**, *122*, 6136.
38. Barreca, M. L.; Lee, K. W.; Chimirri, A.; Briggs, J. M. *Biophys. J.* **2003**, *84*, 1450.
39. Dayam, R.; Neamati, N. *Bioorg. Med. Chem.* **2004**, *12*, 6371.
40. Espeseth, A. S.; Felock, P.; Wolfe, A.; Witmer, M.; Grobler, J.; Anthony, N.; Egbertson, M.; Melamed, J. Y.; Young, S.; Hamill, T.; Cole, J. L.; Hazuda, D. J. *Proc. Natl. Acad. Sci. U.S.A.* **2000**, *97*, 11244.
41. Grobler, J. A.; Stillmock, K.; Binghua, H.; Witmer, M.; Felock, P.; Espeseth, A. S.; Wolfe, A.; Egbertson, M.; Bourgeois, M.; Melamed, J.; Wai, J. S.; Young, S.; Vacca, J.; Hazuda, D. J. *Proc. Natl. Acad. Sci. U.S.A.* **2002**, *99*, 6661.
42. Kawasuji, T.; Fuji, M.; Yoshinaga, T.; Sato, A.; Fujiwara, T.; Kiyama, R. *Bioorg. Med. Chem.* **2006**, *14*, 8420.
43. Katritzky, A. R.; Lang, H.; Lan, X. *Tetrahedron* **1993**, *49*, 7445.
44. Gavezzotti, A. *Cryst. Eng. Commun.* **2008**, *10*, 389.
45. Marchand, C.; Neamati, N.; Pommier, Y. *Methods Enzymol.* **2001**, *340*, 624.

46. Burla, M. C.; Camalli, M.; Carrozzini, B.; Cascarano, G. L.; Giacovazzo, C.; Polidori, G.; Spagna, R. *J. Appl. Crystallogr.* **2003**, *36*, 1103.
47. Sheldrick, G. M. SHELXL97. Program for the Refinement of Crystal Structures; University of Gottingen: Germany, **1997**.
48. Farrugia, L. J. *J. Appl. Crystallogr.* **1999**, *32*, 837.
49. Bruno, I. J.; Cole, J. C.; Edgington, P. R.; Kessler, M.; Macrae, C. F.; McCabe, P.; Pearson, J.; Taylor, R. *Acta Crystallogr.* **2002**, *B58*, 389.
50. Nardelli, M. *J. Appl. Crystallogr.* **1995**, *28*, 659.
51. Carmichael, J.; DeGraff, W. G.; Gazdar, A. F.; Minna, J. D.; Mitchell, J. B. *Cancer Res.* **1987**, *47*, 936.